Case Studies in Thermal Engineering 8 (2016) 51–70

Contents lists available at ScienceDirect

Case Studies in Thermal Engineering

journal homepage: www.elsevier.com/locate/csite

Thermodynamic and economic performance improvement of ORCs through using zeotropic mixtures: Case of waste heat recovery in an offshore platform

M. Kolahi, M. Yari *, S.M.S. Mahmoudi, F. Mohammadkhani

Faculty of Mechanical Engineering, University of Tabriz, Tabriz, Iran

ARTICLE INFO

Article history:
Received 26 March 2016
Received in revised form
24 April 2016
Accepted 1 May 2016
Available online 10 May 2016

Keywords:
Organic Rankine cycle
Zeotropic mixture
Thermodynamic and economic analysis
Specific investment cost
Payback period

ABSTRACT

This paper presents a comparative thermodynamic and economic analysis of two kinds of organic Rankine cycles (ORCs) with pure and zeotropic mixtures for recovering waste heat from the exhaust gases of large diesel engines used in the offshore platforms of phase 12 of South Pars Gas on Persian Gulf. The mixtures of three hydrocarbons with two refrigerants in two cycle arrangements (simple ORC and ORC with internal heat exchanger) at different evaporation temperatures are investigated to optimize three indicators. The results showed that both the energy and exergy efficiencies are maximized at particular mass fractions of refrigerants. The ORC with mixture of R236ea/Cyclohexane (with a ratio of 0.6/0.4) has the best performance as its energy and exergy efficiency are 14.57% and 37.84%, respectively. These values are increased to 16.81% and 40.75%, respectively by adding IHE to system. The minimum amount of the specific investment cost for the most cases is achieved at the mass fractions of 0.1 and 0.5 and it is greater for the ORC with IHE. Also the payback period of investment is calculated for comparison of economic value of systems and it is observed that its amounts for the ORC with IHE are greater than simple one.

1. Introduction

By the growing industrialization over the last decades, global energy consumption has increased to a level never reached before, which has led to many serious environmental problems such as climate changes, air pollution, acid rain and ozone layer depletion. Due to the energy shortage and emission problems, the issues of energy saving and energy efficiency improvement has received more attention recently and has become a field of intense research and development. Utilization of Organic Rankine Cycle (ORC) is one of the proposed solutions to increase the energy usage and to reduce environmental emissions. Waste heat recovery is one of the applications of this system. As an example, by recovering waste heat from exhaust gases of an engine, the efficiency of the engine will be greatly enhanced.

In an ORC, the working fluid is an organic compound instead of water in the traditional steam cycle. Lower boiling point temperature and higher vapor pressure of organic fluids make better conformity with low and medium temperature heat sources compared to water. Also the ORC technology has many other advantages such as possibility of local and small scale power generation, simplicity of components and startup procedure, no need to operator attendance, easy maintenance

* Corresponding author.
E-mail address: myari@tabrizu.ac.ir (M. Yari).

http://dx.doi.org/10.1016/j.csite.2016.05.001

Nomenclature

Abbreviations

CEPCI	chemical engineering plant cost index
GWP	global warming potential
IHE	internal heat exchanger
ODP	ozone depletion potential
ORC	organic Rankine cycle
PP	payback period
SIC	specific investment cost

Greek letters

ΔH_{vap}	heat of vaporization (kJ/kgK)
η	efficiency (%)
μ	dynamic viscosity (Pa s)
ρ	density (kg/m^3)
ε	effectiveness of internal heat exchanger (%)

Symbols

$\dot{E}x$	exergy destruction (kW)
$\dot{E}$	exergy (kW)
$\dot{m}$	mass flow (kg/s)
$\dot{Q}$	heat absorbed or released (kW)
$\dot{W}$	work (kW)
A	heat transfer surface area (m^2)
B_o	boiling number
C	cost (k$)
h	specific enthalpy (kJ/kg) or heat transfer coefficient (W/m^2 K)
k	thermal conductivity (W/mK)
L	length (m)
MM	molar mass (g/mol)
N_u	Nusselt number
P	pressure (MPa)
P_r	Prandtl number
R_e	Reynolds number
s	specific entropy (kJ/kgK)
T	temperature (K)
U	overall heat transfer coefficient (W/m^2 K)
V	velocity (m/s)
x	vapor quality

Subscripts

+IHE	with internal heat exchanger
1*pH*	single phase
2*pH*	two phase
BM	bare module
c	condenser
cd	condensation dew point
cr	critical point
e	evaporator
eb	evaporation bubble point
f	working fluid
g	exhaust gas
I	energy efficiency
i	equipment i
IHE	internal heat exchanger
II	exergy efficiency
in	inlet
l	liquid
LMTD	logarithmic mean temperature difference
net	net output
out	outlet
p	pump
pp, c	condensation pinch point
pp, h	evaporator pinch point
t	turbine
TBM	total bare module
TCI	total capital investment
tot	total
v	vapor
w	cooling water

procedure, long life, lower cost and applicability with various kinds of heat resource. Low thermal efficiency than that of the steam cycle and organic fluid defects (i.e. flammability, toxicity, environmental concerns and their high cost) are the main drawbacks of the ORC technology [1,2]. Therefore, many studies have been accomplished to find suitable organic working fluids for the ORC system. Wang et al. [3] analyzed the performance of the ORC system using nine different pure organic working fluids which has recovered waste heat from internal combustion engines on the vehicles. The results showed that R245fa and R245ca were the most environmentally friendly working fluids. Shu et al. [4] investigated alkanes-based working fluids and found that they may be more attractive for the ORC system in engine exhaust heat recovery. Tian et al. [5] considered twenty low boiling organic fluids and reported that the R141b, R123 and R245fa perform better. Chacartegui [6] analyzed the performance of low temperature ORC by using toluene, cyclohexane, isopentane, isobutene, R113 and R245, and the results showed that the first two perform better. Roy et al. [7] optimized an ORC system with R12, R123, R134a, and R717 as working fluids and found that the ORC with R123 has maximal thermal efficiency as well as minimal irreversibility.

Utilization of the pure fluids including single chemical compounds causes larger irreversibilities in the heat transfer processes due to isothermal temperature profile in the evaporation and condensation. Using of the zeotropic mixtures as working fluid enhance the temperature matching between fluids in heat exchangers and can partly solve this issue. The effects of mixtures used in the ORC are investigated in the work of M. Chys [8]. The results showed that the cycle efficiency increases at the specific heat sources, compared with pure fluids. Wang et al. [9] experimentally investigated the use of zeotropic mixtures and R245fa for a solar ORC and found that the zeotropic mixtures can produce higher collector efficiency and thermal efficiency compared to R245fa in the experimental condition. Heberle et al. [10] examined the performance of isobutane/isopentane and R227ea/R245fa mixtures in a geothermal ORC. Investigation showed that the second law

efficiency of zeotropic mixtures is higher than pure fluids. Bliem [11] compared a geothermal plant efficiency with mixtures and pure fluids and found that the mixture of R114/R22 has 3–8% higher efficiency compared to pure R114.

Reforming the cycle configurations is the other way to improve the performance and the profitability of the system such as regenerative configuration and a system combined with Internal Heat Exchanger (IHE). Shu et al. [12] analyzed the effects of IHE on thermal efficiency and the exergy destruction of ORC with both pure fluids and mixtures. Investigation showed that by adding IHE to system, cycle performance improved, and for benzene/R11 (0.7/0.3) mixture, the efficiency growth is about 7.12% 9.72%. Li et al. [13] compared the thermal and exergy efficiency between the ORC with IHE and simple one and found that the increase in ORC with IHE efficiency were higher for the mixtures R141b/RC318 than for pure R141b. Mago et al. [14] investigated first and second law analysis and compared the regenerative ORC with the simple one and discovered that the regenerative ORC has higher efficiency. Pei et al. [15] analyzed the performance of regenerative ORC compared to simple one for solar thermal electricity generation. The results showed that the maximum efficiency and the maximum overall system efficiency of regenerative ORC are 9.2% and 4.6–5.4% higher than simple one, respectively.

Also, there are many indicators which have used by researchers to analyze the performance of the system. In the study of Roy et al. [16] three indicators, i.e. net power output, first and second law efficiencies, were used for the parametric optimization of a waste heat recovery system based on an ORC. Yari [17] investigated the performance of different ORC configurations such as regenerative ORC with internal heat exchanger, regenerative ORC, ORC with internal heat exchanger and basic ORC using dry organic fluids, with thermal efficiency, exergy efficiency and exergy destruction rate as the performance indicators. Aljundi [18] adopted three indicator parameters, which were thermal efficiency, second law efficiency and mass flow rate to analyze the effects of the working fluid and critical temperature on the performance of ORC and found that the efficiency is a strong function of working fluid's critical temperature. Thermodynamic and economic optimization of an ORC was performed by Quoilin et al. [19] that is employed the total heat recovery efficiency, overall system efficiency and specific investment cost of system to seek the optimal working conditions for the economic optimization with R600, R601, R123, R134a, R1234yf, R245fa, SES36, and HFE7000. The results showed that R600 was the optimal working fluid. Cayer et al. [20] carried out a parametric optimization of a transcritical power cycle using six indicators: net power output, thermal efficiency, exergy efficiency, total surface of the heat exchangers, total heat transfer capacity and relative cost of the system. Shengjun et al. [21] studied the performance of subcritical ORC and transcritical power cycle system using thermal efficiency, exergy efficiency, recovery efficiency, heat exchanger per unit power output and the Levelized Energy Cost, as the performance indicators. Xiao et al. [22] built a multi-objective function by the incorporation of single-objective functions, i.e., net power output, exergy drop of the exhaust gas, total exergy destruction rate and total system cost. The model was optimized using the method of linear weighted evaluation function by the use of pure working fluids R600a, R245fa, R601a, R601, R123, and zeotropic mixed working fluids R600a/R601a, R245fa/R601a, R245fa/R601, R600a/R245fa.

A review of the above literature demonstrates that most of the investigations are concentrated on selecting or mixing working fluids and optimization of the thermodynamic performance or cost of the ORC system. However, still there are only a limited number of researches about the effects of mass fraction of fluids in the zeotropic mixtures especially in the economic field. The aim of this paper is to optimize and compare the thermodynamic and economic potential of simple ORC and ORC with internal heat exchanger using pure and zeotropic mixtures as working fluids under different mass fractions of fluids, for recovering waste heat from the exhaust gases of large diesel engines used in the offshore platforms of phase 12 of South Pars Gas on Persian Gulf. In summary, this paper presents the following specific subjects to the related field of study:

- Investigation of two cycle arrangements at special case: Simple ORC and ORC with IHE for waste heat recovery of offshore diesel engine.
- Utilization of zeotropic mixtures: The mixtures of three hydrocarbons (Hexane, Cyclohexane and Isohexane) with two refrigerants (R236ea and R245fa).
- Consideration of effects of mixtures in heat exchanger designing.
- Optimization of thermodynamic and economic indicators at different mass fractions of refrigerants: Energy efficiency, exergy efficiency and specific investment cost.
- Comparison of economic value of systems using payback period of investment at different mass fractions of refrigerants.
- Examination of effect of evaporation temperature on the indicators at different mass fractions of refrigerants.

2. Systems and working fluids description

2.1. Systems description

Fig. 1 presents two kinds of cycle arrangements for Organic Rankine Cycles (ORCs): a simple ORC and an ORC with Internal Heat Exchanger (IHE). A simple ORC system consists of an evaporator, a turbine, a condenser and a pump, while in the ORC with IHE an internal heat exchanger is added to the cycle to improve the performance of the system. The turbines of two systems are connected through the shaft to the generator to produce electricity.

In the present study, the heat source is the hot exhaust gas of a large diesel engine which is used in offshore platform of South Pars Gas and the heat sink, is considered to be sea (Persian Gulf) water. The other parameters of the ORC systems are given in Table 1.

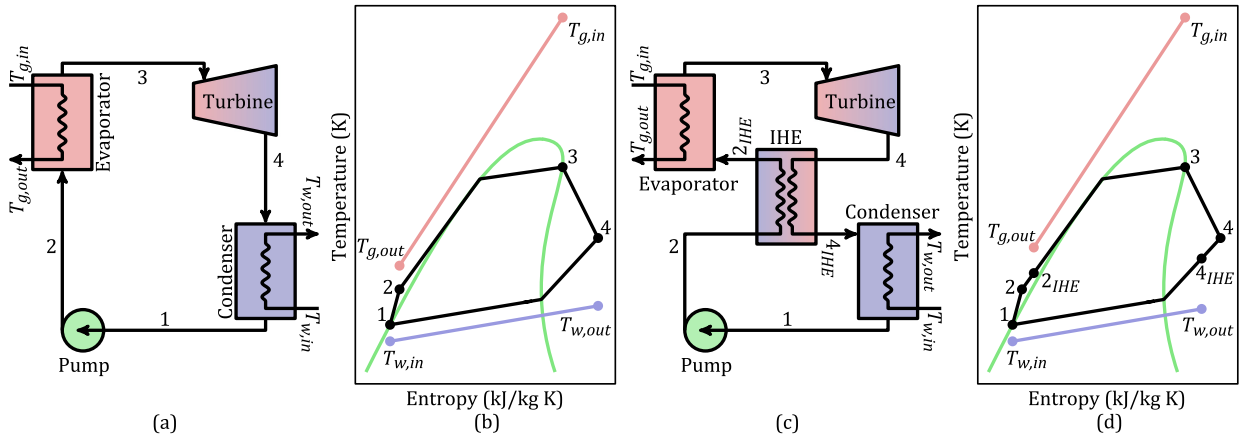

Fig. 1. System diagrams and T-s diagrams of simple ORC and ORC with IHE.

Table 1
Some given parameters for ORC systems. (Parameters of the diesel engine are adopted from Ref. [23]).

Outlet temperature of exhaust gas, $T_{g,in}$ (K)	698.85
Iutlet temperature of cooling water, $T_{w,in}$ (K)	293.15
Evaporation bubble point temperature, T_{eb} (K)	410
Condensation dew point temperature, T_{cd} (K)	328.15
Pressure of exhaust gas, P_g (kPa)	150
Pressure of cooling water, P_w (kPa)	150
Evaporator pinch point temperature difference, $\Delta T_{pp,h}$ (K)	20
Condenser pinch point temperature difference, $\Delta T_{pp,c}$ (K)	10
Exhaust gas mass flow rate, $\dot{m}_g$ (kg/s)	1.2154

The working fluid is pressurized by the pump to a high pressure (1–2). Next, the evaporator, evaporates the pressurized working fluid and converts it to saturated vapor by the heat that absorbed from the hot exhaust gases (2–3). Then, saturated vapor expands to a superheated vapor, by the turbine (3–4), where it delivers work to generate electricity. Finally, the superheat vapor condensed into saturated liquid by the cooling water in the condenser (4–1). In the ORC with IHE, after the pumping process, the pressurized working fluid absorbs heat ($2 - 2_{IHE}$) by the IHE that is recovered from the stage after the turbine ($4 - 4_{IHE}$). Thus the cycles complete. The corresponding $T - s$ diagram of two ORCs are shown in Fig. 1(b) and (d).

2.2. Working fluids candidates

The selection of working fluid of ORC is a very important procedure in the design process of a system. From numerous working fluids there are just a certain number of them can be chosen. Many principles and limitations should be considered when selecting the working fluids for the ORC application. The following guidelines and indicators which are adapted from Quoilin et al. [24], should be taken into account to obtain good selection:

1. Thermodynamic performance: the efficiency and output power should be as high as possible for a given heat source and heat sink temperatures. This performance depends on a number of interdependent thermodynamic properties of the working fluid: critical point, specific heat, density, etc.
2. Positive or isentropic saturation vapor curve (ds/dT): a negative saturation vapor curve (wet fluid) leads to droplets in the later stages of the turbine. The vapor must therefore be superheated at the turbine inlet to avoid turbine damage.
3. High vapor density: lower density leads to higher volume flow rate and the size of the heat exchangers must be increased to limit the pressure drops. This has a non-negligible impact on the cost of the system.
4. Low viscosity and high conductivity: low viscosity and high conductivity in both the liquid and vapor phases result in high heat transfer coefficients and low friction losses in the heat exchangers.
5. High safety level: safety involves two main parameters; toxicity and flammability.
6. Low Ozone Depleting Potential (ODP) and Global Warming Potential (GWP).
7. Good availability and low cost.

However, in general, it is not possible all the considerations to be collected simultaneously in one case. One of the alternative ways to solve this problem is using zeotropic mixtures instead of pure fluids as ORC working fluid.

Using zeotropic mixtures as a working fluid also have another advantage which is obvious temperature glide in the phase

Table 2
The characteristics of the working fluid candidates [18,25].

Fluid	MM (g/mol)	T_{cr} (K)	P_{cr} (MPa)	ODP	GWP	type
R236ea	152.04	412.44	3.502	0	1350	Dry
R245fa	134.05	427.16	3.651	0	1020	Dry
Hexane	86.175	507.82	3.034	0	0	Dry
Cyclohexane	84.161	553.64	4.075	0	Small	Dry
Isohexane	86.175	497.7	3.04	0	Small	Dry

change process at constant pressure. This character of the mixture provides better temperature matching between the temperature profile of the working fluid and the heat source or heat sink media profile. This causes that the outlet temperature of evaporator and condenser, respectively, be higher and lower than that of the pure fluid and consequently increases the cycle efficiency and reduces the exergy destruction of the system.

Finally, three hydrocarbons and two refrigerants are selected to mixing together according to the considerations. The characteristics of the working fluid candidates are described in Table 2.

3. Thermodynamic modeling

For the performance analysis of ORC systems it is necessary to give operating conditions, because of the temperature glide of mixtures during the phase change process. Therefore, the condensation dew point temperature T_{cd} (which is set as cycle condensation temperature), and evaporation bubble point temperature T_{eb} (which is set as evaporation temperature) are considered to be fixed in the present work.

For simplicity in our thermodynamic modeling, the other general assumptions and the initial conditions are described below:

- The all components of the ORC systems operate in the steady state conditions;
- The pressure drops and heat losses in thermodynamic analysis as well as changes in kinetic and potential energies are neglected;
- The irreversibilities in the pipes are negligible;
- The compositions of the mixtures and working fluids do not change during the running process;
- The exhaust gas is supposed as ideal gas and its composition is assumed to be: oxygen = 11.23%, nitrogen = 74.16%, water = 3.0% and carbon dioxide = 11.61%.
- The temperature glide profile of the mixtures is considered to distribute linearly along heat exchangers;
- The ambient temperature and pressure are 298.15 K and 1 atm, respectively;
- The isentropic efficiency of the turbine is 85% and for the pump is 80%. Also the effectiveness of IHE is $\varepsilon = 50\%$.

The thermodynamic modeling of the systems is carried out by MATLAB with a combination of the REFPROP library Version 8.0. [25] to retrieve fluids properties.

According to the first and the second laws of thermodynamics, the energy and exergy analysis are described as follows:

3.1. Energy analysis model

According to the first law of thermodynamics, the following formulas describe the energy behavior of working fluids at any point of the ORC:

Heat absorbed and released in the evaporator and condenser are respectively calculated by:

Without IHE:

$$\dot{Q}_e = \dot{m}_g(h_{g,in} - h_{g,out}) = \dot{m}_f(h_3 - h_2) \quad (1)$$

$$\dot{Q}_c = \dot{m}_w(h_{w,out} - h_{w,in}) = \dot{m}_f(h_4 - h_1) \quad (2)$$

With IHE:

$$\dot{Q}_{e+IHE} = \dot{m}_g(h_{g,in} - h_{g,out}) = \dot{m}_f(h_3 - h_{2_{IHE}}) \quad (3)$$

$$\dot{Q}_{c+IHE} = \dot{m}_w(h_{w,out} - h_{w,in}) = \dot{m}_f(h_{4_{IHE}} - h_1) \quad (4)$$

Heat recovery in the IHE:

$$\dot{Q}_{IHE} = \dot{m}_f(h_{2_{IHE}} - h_2) = \dot{m}_f(h_4 - h_{4_{IHE}}) \quad (5)$$

Turbine power output:

$$\dot{W}_t = \dot{m}_f(h_3 - h_4) = \dot{m}_f(h_3 - h_{4s}) > \eta_t \tag{6}$$

Pump power input:

$$\dot{W}_p = \dot{m}_f(h_2 - h_1) = \dot{m}_f(h_{2s} - h_1)/\eta_p \tag{7}$$

Net mechanical power output:

$$\dot{W}_{net} = \dot{W}_t - \dot{W}_p \tag{8}$$

Thermal efficiency (The first law efficiency):

$$\eta_I = \frac{\dot{W}_{net}}{\dot{Q}_e} \tag{9}$$

And effectiveness of IHE is defined by:

$$\varepsilon = \frac{T_4 - T_{4_{IHE}}}{T_4 - T_2} \tag{10}$$

3.2. Exergy analysis model

On the basis of the second law of thermodynamics, the thermodynamic irreversibility which is occurring generally on each component, can be determined from following formulas:

The exergy for each steady state point of ORCs is defined by:

$$e_x = h_x - h_0 - T_0(s_x - s_0) \tag{11}$$

where 0 subscript mean the reference state (dead state), which is taken as standard state values in this paper (i.e. 25 °C and 1 atm, for the reference temperature and pressure, respectively). It is notable that the chemical exergy has not played a role in analysis since the mass fraction of working fluids is considered constant at all of the cycles.

Exergy supplied by the hot exhaust gases:

$$\dot{E}_g = \dot{m}_g(e_{g,in} - e_{g,out}) \tag{12}$$

Exergy efficiency:

$$\eta_{II} = \frac{\dot{W}_{net}}{\dot{E}_g} \tag{13}$$

Exergy destruction of evaporator and condenser, respectively:

Without IHE:

$$\dot{E}x_e = \dot{m}_g\Big[(h_{g,in} - h_{g,out}) - T_0(s_{g,in} - s_{g,out})\Big] - \dot{m}_f\Big[(h_3 - h_2) - T_0(s_3 - s_2)\Big] \tag{14}$$

$$\dot{E}x_c = \dot{m}_f\Big[(h_4 - h_1) - T_0(s_4 - s_1)\Big] - \dot{m}_c\Big[(h_{w,out} - h_{w,in}) - T_0(s_{w,out} - s_{w,in})\Big] \tag{15}$$

With IHE:

$$\dot{E}x_{e_{+IHE}} = \dot{m}_g\Big[(h_{g,in} - h_{g,out}) - T_0(s_{g,in} - s_{g,out})\Big] - \dot{m}_f\Big[(h_3 - h_{2_{IHE}}) - T_0(s_3 - s_{2_{IHE}})\Big] \tag{16}$$

$$\dot{E}x_{c_{+IHE}} = \dot{m}_f\Big[(h_{4_{IHE}} - h_1) - T_0(s_{4_{IHE}} - s_1)\Big] - \dot{m}_c\Big[(h_{w,out} - h_{w,in}) - T_0(s_{w,out} - s_{w,in})\Big] \tag{17}$$

Exergy destruction of IHE:

$$\dot{E}x_{IHE} = \dot{m}_f T_0(s_{2_{IHE}} - s_2 + s_{4_{IHE}} - s_4) \tag{18}$$

Turbine exergy destruction rate:

$$\dot{E}x_t = \dot{m}_f T_0(s_4 - s_3) \tag{19}$$

Table 3
Comparison between the results of this study and Ref. [12].

	Ref. [12]	This study	Deviation
Heat input			
$\dot{Q}_e$(kW)	124.96	124.84	0.10%
$\dot{Q}_{e_{+IHE}}$(kW)	121.39	121.12	0.22%
Energy efficiency			
η_I (%)	13.73	13.69	0.29%
$\eta_{I_{+IHE}}$ (%)	15.94	15.91	0.19%
Total exergy destruction			
$\dot{E}x_{tot}$ (kW)	32.12	32.02	0.31%
$\dot{E}x_{tot_{+IHE}}$ (kW)	31.04	30.96	0.26%

Pump exergy destruction rate:

$$\dot{E}x_p = \dot{m}_f T_0 (s_2 - s_1) \tag{20}$$

And the cycle total exergy destruction is equal to the sum of its component exergy destructions:
Without IHE:

$$\dot{E}x_{tot} = \dot{E}x_p + \dot{E}x_e + \dot{E}x_t + \dot{E}x_c \tag{21}$$

With IHE:

$$\dot{E}x_{tot_{+IHE}} = \dot{E}x_p + \dot{E}x_e + \dot{E}x_t + \dot{E}x_c + \dot{E}x_{IHE} \tag{22}$$

3.3. Thermodynamic validation

In order to validate the present model, a thermodynamic analysis of the ORC is performed under the same operating conditions as those in Shu et al. [12]. Table 3 shows a good agreement between the present solutions and results from Ref. [12]. The small differences are mainly due to the various versions of REFPROP used in the studies.

4. Economic modeling

4.1. Economic correlations

The capital cost for a plant (such as ORC) must take into consideration many costs other than the purchased cost of the equipment, as described in Turton et al. [26]. It should be noted that all the data for the purchased cost of equipment that adapted from Turton et al. [26] were obtained from a survey of equipment manufacturers in the year of 2001, with an average value of the CEPCI (Chemical Engineering Plant Cost Index) of 397. Therefore, the updated value of 576.1 of CEPCI for the year of 2014 is used in this paper [27].

The following equations present some of the cost correlations that applied in the evaluation of the total capital investment which are adapted from Seider et al. [28].

$$C_{TBM} = \sum C_{BM_i} \tag{23}$$

$$C_{site} = 0.05 C_{TBM} \tag{24}$$

$$C_{serv} = 0.05 C_{TBM} \tag{25}$$

$$C_{DPI} = C_{TBM} + C_{site} + C_{serv} \tag{26}$$

$$C_{cont} = 0.18 C_{DPI} \tag{27}$$

$$C_{TDC} = C_{DPI} + C_{cont} \tag{28}$$

$$C_{startup} = 0.1 C_{TDC} \tag{29}$$

Table 4
Constants for the cost calculations [26].

Equipments	K_{1_i}	K_{2_i}	K_{3_i}	C_{1_i}	C_{2_i}	C_{3_i}	B_{1_i}	B_{2_i}	F_{M_i}	F_{BM_i}
Pump	3.3892	0.0536	0.1538	−0.3935	0.3957	−0.00226	1.89	1.35	1.6	–
heat exchanger	4.3247	−0.303	0.1634	0.03881	−0.11272	0.08183	1.63	1.66	1.0	–
Turbine	2.2476	1.4965	−0.1618	–	–	–	–	–	–	6.1
Electrical generator	–	–	–	–	–	–	–	–	–	1.5

$$C_{TCI} = C_{TDC} + C_{startup} \tag{30}$$

where C_{TBM} is total bare module cost; C_{BM_i} is bare module equipment cost; C_{site} is cost of site preparation; C_{serv} is the cost of service facilities; C_{DPI} is total direct permanent investment; C_{cont} is cost of contingencies and the contractor's fee; C_{TDC} is total depreciable capital; $C_{startup}$ is cost of plant startup; and C_{TCI} is total capital investment.

The bare module cost is the sum of the direct and indirect costs. The Eq. (31) is used to calculate the bare module cost for each piece of equipment:

$$C_{BM_i} = C^0_{p_i} F_{BM_i} \tag{31}$$

where C_{BM_i} is bare module equipment cost: sum of direct and indirect costs for each unit; $C^0_{p_i}$ is purchased the cost for base conditions: equipment made of the most common material, usually carbon steel and operating at near ambient pressures; and F_{BM_i} is bare module cost factor [26].

The purchased equipment cost for base conditions, $C^0_{p_i}$, is calculated by:

$$\log_{10} C^0_{p_i} = K_{1_i} + K_{2_i} \log_{10}(A_i) + K_{3_i}\left[\log_{10}(A_i)\right]^2 \tag{32}$$

where A_i is a dimensional parameter corresponding to the surface area for heat exchangers or work for pump, turbine and electrical generator. The mechanical work of pump or turbine can be obtained by the Eqs. (7) and (6). The electrical work of the generator is considered to be $\dot{W}_g = 0.95\dot{W}_t$. Also the heat exchangers surface area calculations are presented in Section 4.2.

Bare module factors, F_{BM_i}, for pumps and heat exchangers are calculated by the Eq. (33); and for the other equipment are given in Table 4.

$$F_{BM_i} = B_{1_i} + B_{2_i} F_{M_i} F_{P_i} \tag{33}$$

where the values of the constants B_{1_i} and B_{2_i} and equipment material factor, F_{M_i}, are given in Table 4.

F_{P_i} is operating pressure factor and is obtained by the following equation:

$$\log_{10} F_{p_i} = C_{1_i} + C_{2_i} \log_{10}(P_i) + C_{3_i}\left[\log_{10}(P_i)\right]^2 \tag{34}$$

The constants C_{1_i}, C_{2_i} and C_{3_i} are given in Table 4 and the units of pressure in this equation, are bar gauge or barg (1 bar=0.0 barg). The pressure factors are always greater than unity.

Finally, for the economic optimization, the Specific Investment Cost (SIC) that represents the ratio of the total capital investment, C_{TCI}, to the net power output, $\dot{W}_{net}$, for the ORC system is defined as:

$$SIC = \frac{C_{TCI}}{\dot{W}_{net}} \tag{35}$$

The other parameter which gives a better intuition of the economic analysis is Payback Period (PP) of investment. The payback period is defined as the length of time required for the cash inflows received from a project to recover the original cash outlays required by the initial investment, and it can be calculated by dividing the total depreciable capital by the average annual net cash inflow (ANCF) [29]:

$$PP = \frac{C_{TDC}}{ANCF} \tag{36}$$

where $ANCF = 0.1(\$/\text{kWh}) \cdot \dot{W}_g(\text{kW}) \cdot 7446(\text{h/year})$, in which $0.1(\$/\text{kWh})$ is electricity price for selling to the network of corresponding case [30], $\dot{W}_g$ is the electrical work of the generator and 7446 $(= 0.85 \times 24 \times 365)$ is annual operating hours of the systems.

4.2. Heat exchanger surface area calculations

The shell and tube heat exchangers with approximate counterflow pattern are chosen for the evaporator, condenser and IHE in this work. The generic geometry of shell and tube heat exchanger is shown in Fig. 2 and several parameters of heat exchangers are given in Table 5, while several other parameters such as the number of tubes and baffle cuts should be

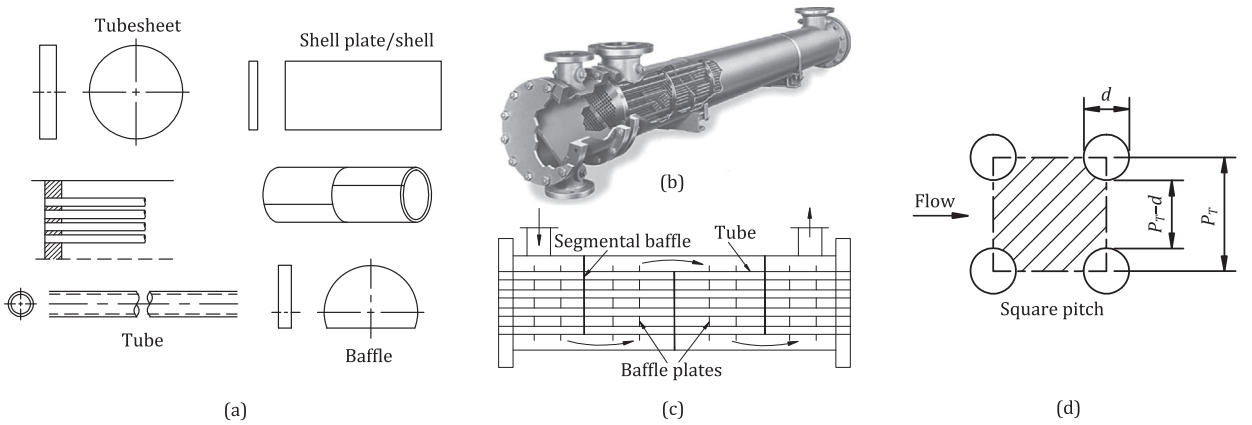

Fig. 2. (a) Major components of a shell and tube heat exchanger. (b) Cut section of a shell and tube heat exchanger. (c) NTIW design. (d) Flow area of square pitch; [31].

Table 5
Some given parameters for heat exchangers.

Outer tube diameter, d_o (cm)	2.54
Inner tube diameter, d_i (cm)	2.3622
Tube pitch, P_T (cm)	3.175
Number of tube passes, N^t_P	2

modified later to satisfy the pressure constraints.

The heat exchangers are modeled using the Logarithmic Mean Temperature Difference (LMTD) method in this study:

$$\dot{Q} = UAF\Delta T_{LMTD} \tag{37}$$

where U is the overall heat transfer coefficient; A is the heat transfer surface area; F is the correction factor which is considered to be 1 for phase change processes and 0.95 for other parts; and ΔT_{LMTD} is the logarithmic mean temperature difference.

$$\Delta T_{LMTD} = \frac{(T_{h,out} - T_{c,in}) - (T_{h,in} - T_{c,out})}{\ln\left[(T_{h,out} - T_{c,in})/(T_{h,in} - T_{c,out})\right]} \tag{38}$$

$$U = \left[\frac{d_o}{h_i d_i} + \frac{R_{f_i} d_o}{d_i} + \frac{d_o \ln(d_o/d_i)}{2k} + R_{f_o} + \frac{1}{h_o}\right]^{-1} \tag{39}$$

where d_i and d_o are inner and outer diameters of tubes which are given in Table 5; k is the thermal conductivity of fluids; h_i and h_o are heat transfer coefficient at inside and outside of tubes; R_{f_i} and R_{f_o} are fouling factors at inside and outside of tubes, respectively. The amounts of thermal conductivity and fouling factors can be found in Ref. [32]. Also tube diameters are in B. W.G. 20 standard [33].

In the IHE there is just one phase fluid flow in tubes and shell side, the liquid phase flows inside the tubes and the gas phase is in the shell side. But in the evaporator and condenser there are two zone of fluid flow in tubes: single phase fluid flow and two phase. The working fluid flows inside the tubes and exhaust gas or cooling water around them. The total heat transfer area is the sum of the heat transfer areas of the two zones:

$$A_{tot} = A_{1pH} + A_{2pH} \tag{40}$$

In the surface area calculations, it is necessary to know the number of tubes of the heat exchangers. To reduce the cost of heat exchangers the number of tubes should be minimized, but the pressure drop considerations should be taken into account. Thus, the pressure drop correlations are presented in Appendix A.

The shell side heat transfer coefficient of evaporator, condenser and IHE is calculated by the Bell-Delaware method [34]. It should be noticed that the fluid flow of all of these sides is in the single phase. As described in Ref. [34]:

$$h_{shell_{1pH}} = h_{id} J_c J_l J_b J_s J_r \tag{41}$$

where h_{id} is the heat transfer coefficient for pure cross-flow in an ideal tube bank; J_c is a correction factor for baffle window flow; J_l is the correction factor for baffle leakage effects; J_b is the correction factor for bundle bypass effects; J_r is the laminar

flow correction factor; J_s is the correction factor for unequal baffle spacing. The combined effect of all these correction factors for a reasonable well-designed shell-and-tube heat exchanger is approximately 0.6 [35].

The heat transfer coefficient for pure cross-flow in an ideal tube bank, h_{id}, is calculated by [35]:

$$h_{id} = j_i \; Cp_s \left(\frac{\dot{m}_s}{A_s}\right)\left(\frac{k_s}{Cp_s \; \mu_s}\right)^{2/3}\left(\frac{\mu_s}{\mu_s^w}\right)^{0.14} \tag{42}$$

where j_i is the Colburn j-factor for an ideal tube bank, which is calculated in Appendix B.

Heat transfer coefficient of single phase flow of evaporator, condenser and IHE in smooth tubes is predicted by the Gnielinski correlation [36], that is valid for $0.5 \le Pr \le 2000$ and $3 \times 10^3 \le Re \le 5 \times 10^6$:

$$h_{tube_{1pH}} = Nu \; \frac{k}{D} \tag{43}$$

where Nu is the Nusselt number:

$$Nu = \frac{(f/8)(Re - 1000)Pr}{1 + 12.7(f/8)^{0.5}\left(Pr^{2/3} - 1\right)} \tag{44}$$

The two phase flow regions in evaporator and condenser based on discretization method, are divided into n small sections (50 segments in the present work), because of change in fluid properties within a narrow range of temperature and pressure in the two phase flow heat transfer process. This method is subjected to an identical heat transfer rate $\Delta\dot{Q}$ for heat transfer calculation.

The heat transfer coefficient of flow boiling process in horizontal tubes of evaporator, is predicted by the correlation of Gungor-Winterton [37]:

$$h_{tube_{2pH,ev}} = E \; h_l \tag{45}$$

where h_l is single phase liquid flow heat transfer coefficient and E is the enhancement factor which are presented in Appendix B. However, the Gungor-Winterton correlation enhancement factor with the mixture effects is:

$$E = 1 + 3000(BoF_C)^{0.86} + 1.12\left(\frac{x}{1-x}\right)^{0.75}\left(\frac{\rho_l}{\rho_v}\right)^{0.41} \tag{46}$$

The heat transfer coefficient for the condensation process in plain tubes, is predicted by the correlation of Shah [38]. According to this empirical correlation, there are two heat transfer regimes during the condensation in plain tube:

In regime I (turbulent regime)

$$h_{tube_{2pH,co}} = h_I \tag{47}$$

In regime II (mixed regime)

$$h_{tube_{2pH,co}} = h_I + h_{Nu} \tag{48}$$

To correct the predictions of Shah [38] for mixture condensation in plain tubes, Bell and Ghaly [39] method is used. According to this method:

$$\frac{1}{h_{mix}} = \frac{1}{h_{mono}} + \frac{Y_V}{h_{VS}} \tag{49}$$

where

$$Y_V = xCp_v \; \frac{\Delta T_{glide}}{\Delta H_{vap}} \tag{50}$$

h_{mono} is the condensing heat transfer coefficient calculated with mixture properties using the Shah correlation for pure fluids.

And h_{VS} is the superficial heat transfer coefficient of the vapor phase, assuming vapor phase to be flowing alone in the tube, calculated by:

$$h_{VS} = 0.023\left(\frac{GxD}{\mu_v}\right)^{0.8}\frac{(Pr_v)^{0.4}k_v}{D} \tag{51}$$

The other essential correlations are given in appendices.

Table 6
Comparison between the SIC of this study and Ref. [40].

Mass fraction of refrigerant:	0.2	0.4	0.6
SIC ($/kW) of Ref. [40]:	4157	4202	4243
SIC ($/kW) of this study:	3619	4243	3723
Root mean square error:	11.79%		

4.3. Economic validation

Table 6 shows the results of economic validation. To this validation, the work of Le et al. [40] is chosen. However, all of the required data for heat exchanger designing are not presented in this paper. So it is necessary to design them again based on the pressure drop limitation. The differences in the results between the present solutions and those from Ref. [40] are because of this issue.

5. Results and discussion

There are three indicators which are used to investigate the performance of the systems in this paper: the energy efficiency, the exergy efficiency and the specific investment cost. Also, the simulation showed that the evaporation temperature is one of the most important parameters that affects the performance of systems. For this reason, a comprehensive parametric study is finally performed to investigate the effects of this parameter on the performance.

5.1. Thermodynamic and economic analysis

Fig. 3 presents the temperature glides of working fluids in the evaporation and condensation processes of the both simple ORC and ORC with IHE. As this figure shows, there is no difference between temperature glides for the same processes of the systems. The reason is that the condensation and evaporation temperatures are fixed in the simulation. Also, this figure shows that the temperature glides are maximized at particular mass fractions of the refrigerants. As the mass fraction is close to 0 or 1, the working fluid properties become closer to a pure fluid and the glide is reduced.

5.1.1. Thermodynamic analysis

Energy efficiency and exergy efficiency are the most important thermodynamic indexes which are used to investigate the cycle performance. Fig. 4 illustrates the variations of energy efficiency and exergy efficiency as a function of the mass fraction of refrigerants for the both systems. According to this figure, the efficiencies of R236ea/Cyclohexane mixture are higher than the other mixtures. Also, it can be seen that with increasing the mass fraction of refrigerants, both of the efficiencies at all cases, firstly increases, then decreases and the maximum of efficiencies usually occur in the mass fractions of 0.5 or 0.6. As Fig. 3 shows, the temperature glides are also maximized at these fractions which causes better temperature matching between the temperature profile of the working fluid and the heat source or heat sink media profile. Furthermore, it caused the average evaporation temperature and the average condensation temperature of the mixture be higher and lower than that of the pure fluid, respectively. This decreases the exergy destruction and consequently increases the efficiency.

Also, it is apparent from Fig. 4 that the efficiencies of ORC with IHE are obviously higher than the simple one. By preheating fluid at the pump outlet with the superheated vapor of the turbine outlet, IHE recovers part of the heat energy and decline the heat load of the evaporator. In addition, higher and lower temperature of fluid at the inlet of the evaporator and condenser respectively, lead to higher average evaporation temperature and lower average condensation temperature in the ORC with IHE compared to simple ORC. These reasons result higher efficiencies for the ORC with IHE.

The variations of net power output and exergy destruction as a function of the mass fraction of refrigerants are given in Fig. 5. As it is shown, the mixture of R236ea/Cyclohexane has the best performance (i.e. higher net power output and lower exergy destruction) than other mixtures at all cases. In addition, from Fig. 5 there is an optimum value in each case which is usually occurs in the mass fractions of 0.5 or 0.6. In other words, by increasing of the mass fraction of refrigerants, the net power output firstly increase and then decrease but the trend for exergy destruction is reverse. These trends confirm

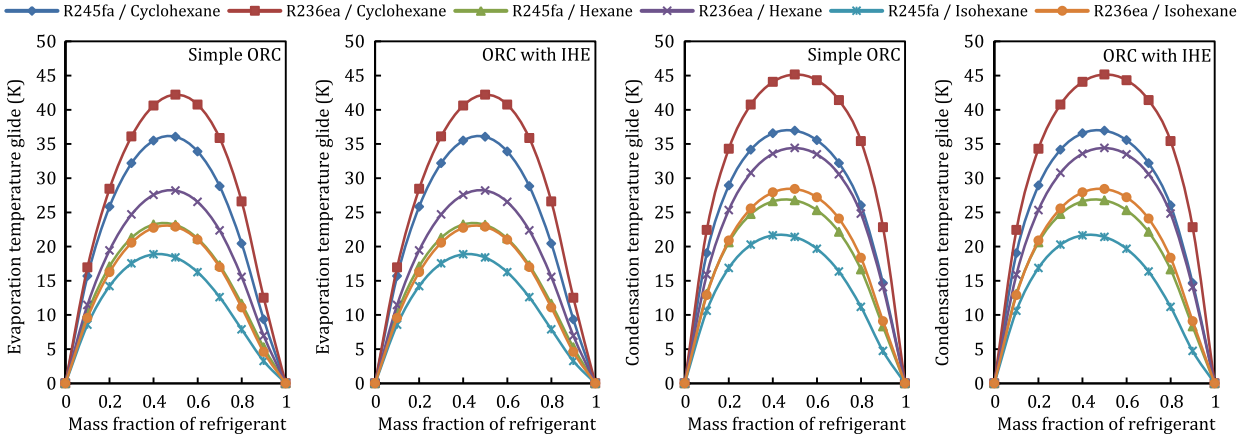

Fig. 3. Temperature glide of different mixtures vs. mass fraction.

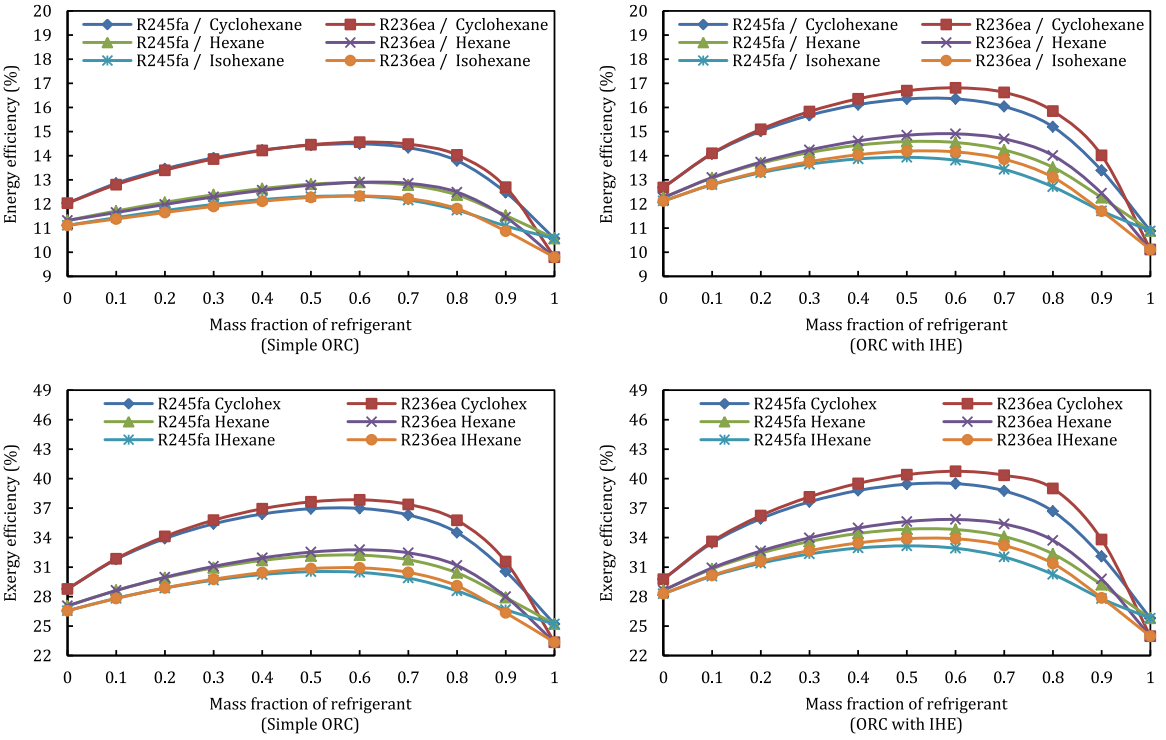

Fig. 4. Energy efficiencies and exergy efficiencies vs. mass fraction.

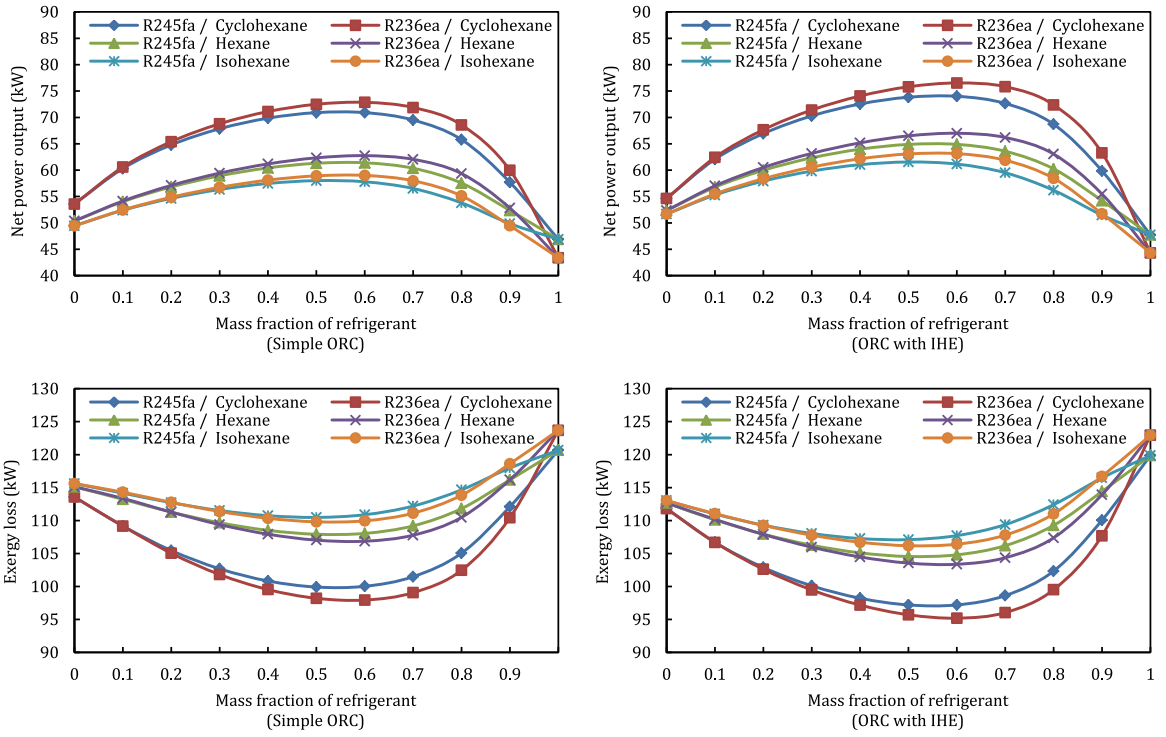

Fig. 5. Net power output and exergy destruction vs. mass fraction.

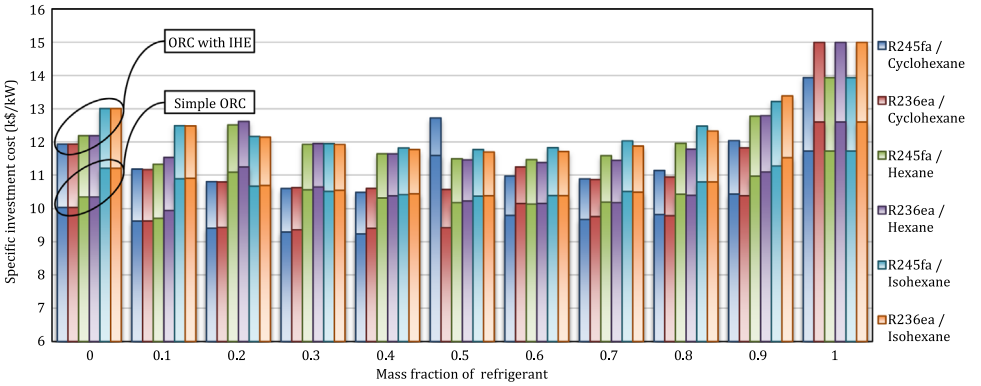

Fig. 6. Specific investment costs of the systems vs. mass fraction.

the variation of energy and exergy efficiencies (see Fig. 3). Although, it is expected to acquire a better performance by adding IHE to the system, however the enhancement does not look striking, as shown in Fig. 5.

5.1.2. *Economic analysis*

One of the most important factors affecting the selection of a design for a thermal system is the cost of the final product (s) [29]. This part focuses on the economic analysis and the Specific Investment Cost (SIC) is selected as a criteria for the investigation. Fig. 6 illustrates the variation of the specific investment cost as a function of the mass fraction of refrigerants for the both systems. As it can be seen, there is an irregularity in the charts. However, the minimum amounts of SIC in the most cases are apparent at the mass fractions of 0.1 or 0.5. In details, the relevant mass fractions for the minimum SIC are: R236ea/Cyclohexane (Simple ORC: 0.3/0.7 and ORC with IHE: 0.5/0.5), R245fa/Cyclohexane (both: 0.4/0.6), R245fa/Hexane (both: 0.1/0.9), R236ea/Hexane (Simple ORC: 0.1/0.9 and ORC with IHE: 0.6/0.4), R245fa/Isohexane (both: 0.5/0.5), R236ea/Isohexane (both: 0.5/0.5). In addition, from Fig. 6, the specific investment costs of the IHE system are greater than the simple one that is because of the existence of an extra heat exchanger in the system.

The Payback Period (PP) of the systems are presented in Fig. 7. As it is shown, the behavior of PP at various amounts of mass fractions of refrigerants are coincident with the behavior of SIC as a function of the mass fraction. Also, it can be seen that the PP of the ORC with IHE whose total capital investment is higher, is greater than simple one, as it is expected. However differences of PPs of the systems are less than 1.5 year at some cases and its minimum amounts are appeared in the mass fractions of 0.4, 0.5 or 0.6. Also, the mixture of R236ea/Cyclohexane has the least differences, and these are because of better power generation in the systems at these cases. Although, the time value of money is not considered by the PP, however utilization of this parameter is a simple way to rank and compare various projects to choose a system with the shortest payback period.

The optimal thermodynamic and economic results for both of the systems are given in Table 7. The mixture of R236ea/Cyclohexane (0.6/0.4) has the best thermodynamic performances, whose energy and exergy efficiencies are 14.57% and 37.84% and they are increased to 16.81% and 40.75%, respectively, by adding IHE to the ORC. Also, the minimum of SIC and PP are 9.24(k$/kW) and 11.75 year for the mixture of R245fa/Cyclohexane (0.4/0.6) and they are increased to 10.48 (k$/kW) and 13.34 year by adding IHE to the system.

5.2. *Effects of the evaporation temperature*

Due to performance analysis of ORC systems, the evaporation temperature is considered to be fixed (410 K) in the previous section. However, as it is mentioned, the evaporation temperature is one of the most important parameters of the systems that affects the thermodynamic and economic performance. Therefore, the effects are examined in this section. The investigation is performed for three mass fractions of refrigerants (0.3, 0.5 and 0.7).

The variations of the energy efficiency, the exergy efficiency and the Specific Investment Cost (SIC) with the evaporation temperature are presented in Figs. 8, 9 and 10, respectively. These figures show that increasing the turbine inlet pressure increases the energy and exergy efficiencies while decreases the specific investment cost. Also, it is apparent that, the ORC with IHE has a better thermodynamic performance but it has more cost. As an important result, the both systems in the mass fraction of 0.5 have better performance. This shows the advantage of using a zeotropic mixture instead of pure fluids as working fluid.

The main consequence of this section is the enhancement of indicators in the most cases with the increasing of evaporation temperature. So it is better to have a greater evaporation temperature.

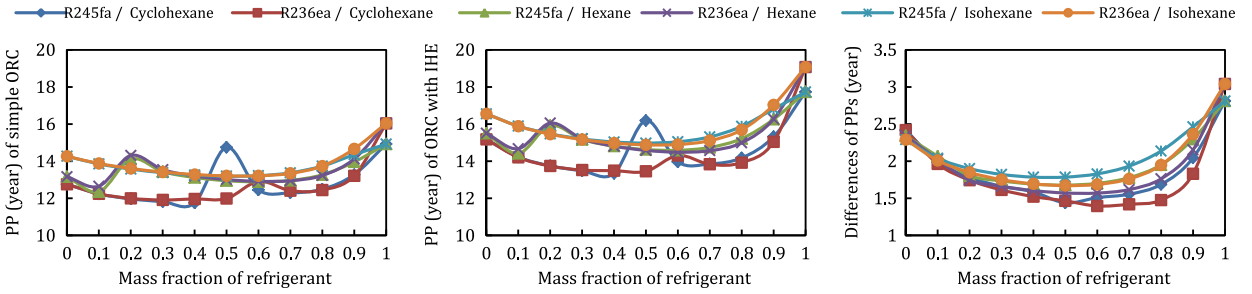

Fig. 7. Payback period of the systems vs. mass fraction.

Table 7
The optimal thermodynamic and economic results for the ORC systems.

	R245fa/Cyclohexane	R236ea/Cyclohexane	R245fa/Hexane	R236ea/Hexane	R245fa/Isohexane	R236ea/Isohexane
Thermodynamic optimal results						
η_I (%)	14.49 (0.6/0.4)	14.57 (0.6/0.4)	12.89 (0.6/0.4)	12.90 (0.6/0.4)	12.32 (0.6/0.4)	12.33 (0.6/0.4)
$\eta_{I_{+IHE}}$ (%)	16.36 (0.6/0.4)	16.81 (0.6/0.4)	14.59 (0.5/0.5)	14.91 (0.6/0.4)	13.94 (0.5/0.5)	14.19 (0.5/0.5)
η_{II} (%)	36.97 (0.6/0.4)	37.84 (0.6/0.4)	32.22 (0.6/0.4)	32.76 (0.6/0.4)	30.53 (0.5/0.5)	30.92 (0.6/0.4)
$\eta_{II_{+IHE}}$ (%)	39.49 (0.6/0.4)	40.75 (0.6/0.4)	34.86 (0.5/0.5)	35.84 (0.6/0.4)	33.16 (0.5/0.5)	33.89 (0.5/0.5)
$\dot{W}_{net}$ (kW)	70.91 (0.6/0.4)	72.86 (0.6/0.4)	61.39 (0.6/0.4)	62.75 (0.6/0.4)	58.01 (0.5/0.5)	59.00 (0.6/0.4)
$\dot{W}_{net_{+IHE}}$ (kW)	74.00 (0.6/0.4)	76.53 (0.6/0.4)	64.88 (0.6/0.4)	66.99 (0.6/0.4)	61.54 (0.5/0.5)	63.13 (0.6/0.4)
$\dot{E}x_{tot}$ (kW)	99.92 (0.5/0.5)	97.94 (0.6/0.4)	107.92 (0.5/0.5)	106.87 (0.6/0.4)	110.48 (0.5/0.5)	109.81 (0.5/0.5)
$\dot{E}x_{tot_{+IHE}}$ (kW)	97.20 (0.5/0.5)	95.20 (0.6/0.4)	104.55 (0.5/0.5)	103.37 (0.6/0.4)	107.11 (0.5/0.5)	106.19 (0.5/0.5)
Economic optimal results						
SIC (k$/kW)	9.24 (0.4/0.6)	9.36 (0.3/0.7)	9.71 (0.1/0.9)	9.94 (0.1/0.9)	10.37 (0.5/0.5)	10.38 (0.5/0.5)
SIC_{+IHE} (k$/kW)	10.48 (0.4/0.6)	10.57 (0.5/0.5)	11.33 (0.1/0.9)	11.38 (0.6/0.4)	11.77 (0.5/0.5)	11.70 (0.5/0.5)
PP (year)	11.75 (0.4/0.6)	11.91 (0.3/0.7)	12.35 (0.1/0.9)	12.65 (0.1/0.9)	13.19 (0.5/0.5)	13.21(0.5/0.5)
PP_{+IHE} (yera)	13.34 (0.4/0.6)	13.45 (0.5/0.5)	14.42 (0.1/0.9)	14.48 (0.6/0.4)	14.98 (0.5/0.5)	14.88 (0.5/0.5)
$\Delta PP = PP_{+IHE} - PP$ (yera)	1.44 (0.5/0.5)	1.40 (0.6/0.4)	1.68 (0.5/0.5)	1.57 (0.6/0.4)	1.78 (0.4/0.6)	1.67 (0.5/0.5)

The numbers in parenthesis in front of the values show the corresponding mass fractions of fluids.

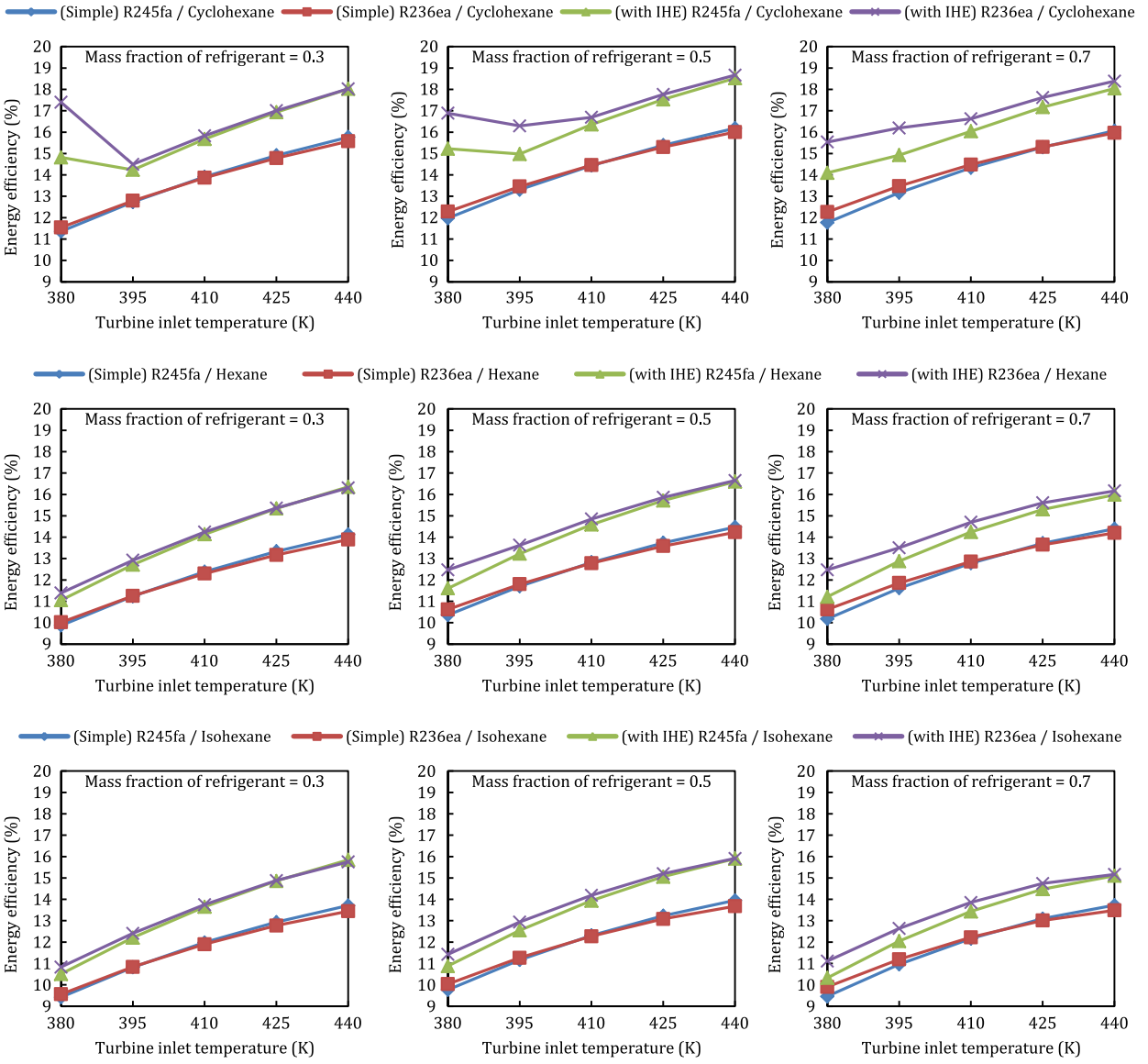

Fig. 8. Energy efficiency vs. evaporation temperature.

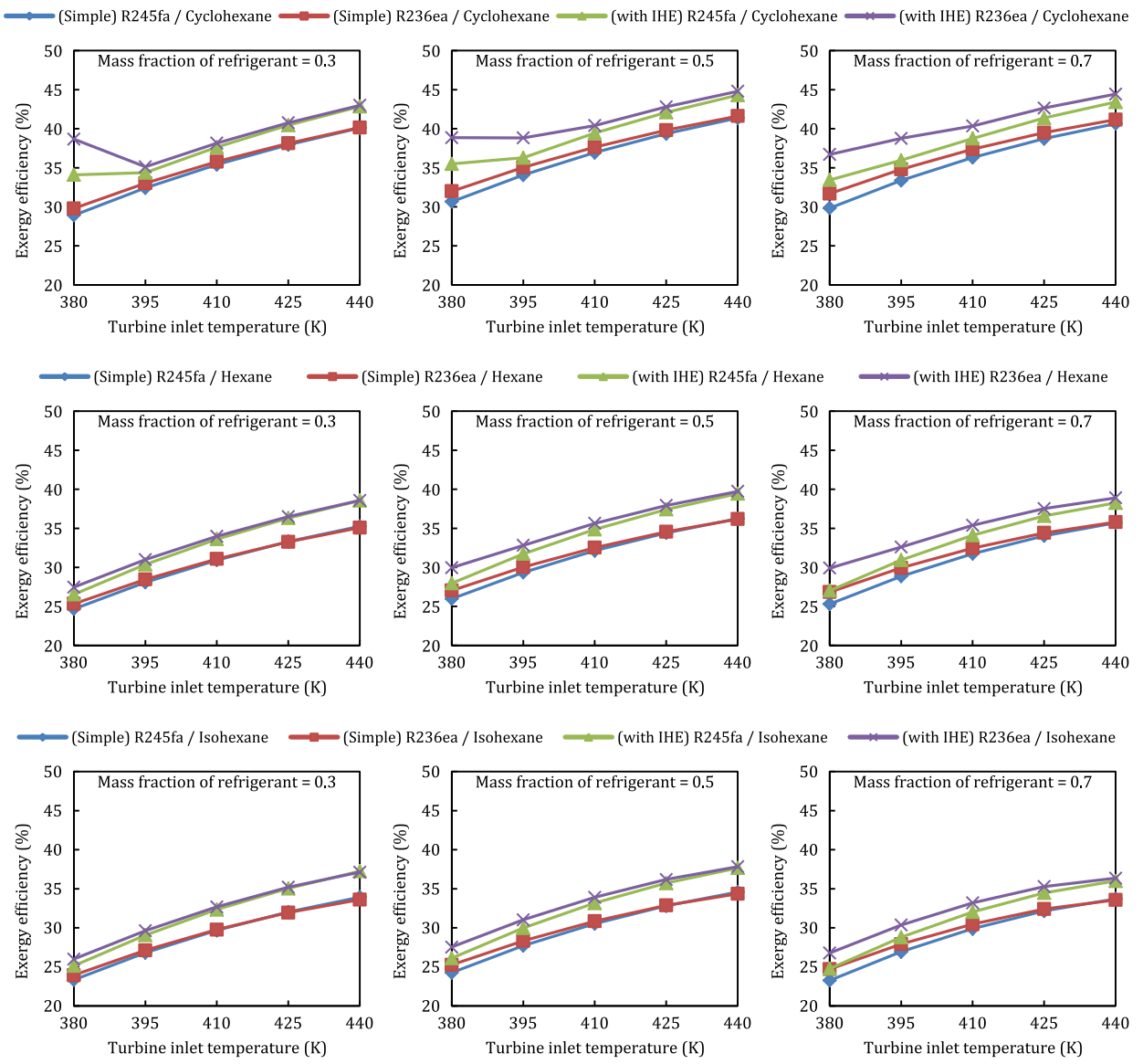

Fig. 9. Exergy efficiency vs. evaporation temperature.

6. Conclusions

The present paper provides the thermodynamic and economic comparison and optimization of the simple ORC and ORC with IHE using zeotropic mixtures utilizing for waste heat recovery from the exhaust gases of large diesel engines used in the offshore platforms of South Pars Gas on Persian Gulf. Energy and exergy efficiencies as well as the specific investment cost of the cycles are investigated. The following conclusions can be drawn:

1. Energy efficiency and exergy efficiency of the R236ea/Cyclohexane mixture at the most mass fractions of refrigerant (R236ea) is higher than other mixtures.
2. With increasing of the mass fraction of refrigerants, both of the efficiencies (i.e. energy efficiency and exergy efficiency) at all cases, firstly increases, then decreases and the maximum of efficiencies usually occur in the mass fractions of 0.5 or 0.6.
3. The efficiencies of the ORC with IHE are higher than the simple one.
4. The minimum amounts of the specific investment cost are apparent at the mass fractions of 0.1 and 0.5 for the most cases and they are greater for the ORC with IHE.
5. The behavior of payback period at various amounts of mass fractions of refrigerants are coincident with the behavior of SIC as a function of the mass fraction, and its amounts for the ORC with IHE are greater than simple one.
6. The maximum energy efficiency is for the mixture of R236ea/Cyclohexane (0.6/0.4) and it is increased from 14.57% to

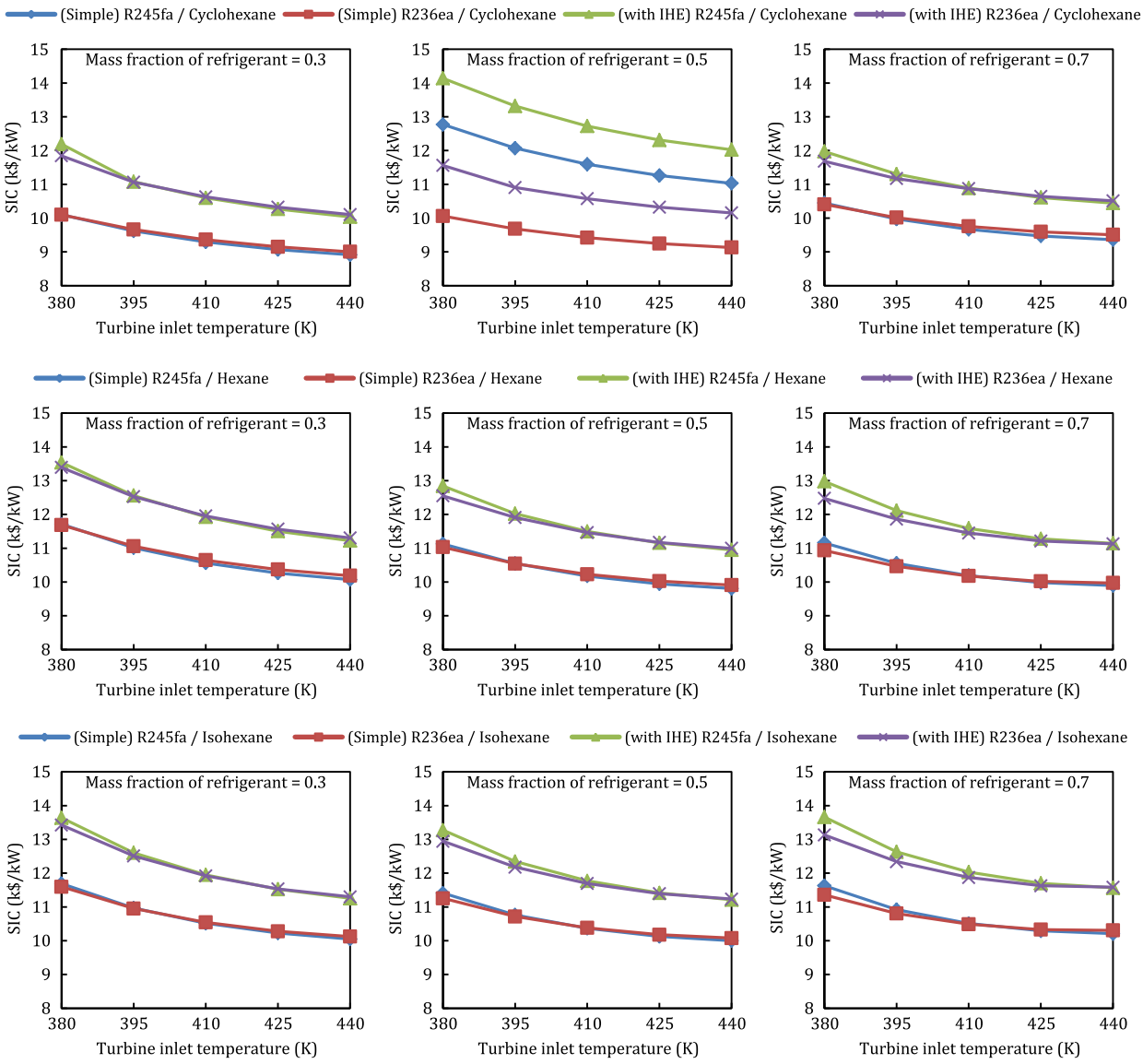

Fig. 10. Specific investment cost vs. evaporation temperature.

16.81% by adding IHE to the ORC system. Also, its maximum exergy efficiency is 37.84% in the simple ORC and 40.75% in the ORC with IHE.

7. The minimum of SIC and PP are 9.24 (k$/kW) and 11.75 year for the mixture of R245fa/Cyclohexane (0.4/0.6) and they are increased to 10.48 (k$/kW) and 13.34 year by adding IHE to the system.
8. By increasing the evaporation temperature, the energy and exergy efficiencies increase and the specific investment cost decreases.

Acknowledgements

The authors would like to gratefully acknowledge S. Hadi Mirbagheri (PETROPARS) for providing the data of diesel engines which are used in the offshore platforms of phase 12 of South Pars Gas.

Appendix A. Pressure drop calculations

The pressure drop allowance in heat exchangers at shell side is 0.5 bar and at the tube side is 0.2 bar [35]. Therefore, with the trial and error method, the minimum number of tubes in the shell with the allowable pressure drop can be found by the following correlations:

The shell side pressure drop [35]:

$$\Delta P_{shell} = \frac{f G_s^2 (N_b + 1) D_s}{2\rho D_e \left(\mu_s/\mu_s^{\,w}\right)^{0.14}} \tag{A.1}$$

where N_b is the number of baffles:

$$N_b = L/b - 1 \tag{A.2}$$

G_s is the shell side mass velocity:

$$G_s = \dot{m}/A_s \tag{A.3}$$

A_s is the bundle cross flow area

$$A_s = (D_s C B)/P_T \tag{A.4}$$

D_e is the shell side equivalent diameter, which is calculated for square tube pitch:

$$D_e = \frac{4\left(P_T^2 - \pi\, d_o^2/4\right)}{\pi\, d_o} \tag{A.5}$$

And f is the friction factor for the shell which is valid for $400 \le Re \le 10^6$:

$$f = \exp\left[0.579 - 0.19 \ln(Re_s)\right] \tag{A.6}$$

The total pressure drop for tube side for single phase fluid [35]:

$$\Delta P_{tube_{1pH}} = \left(f \frac{LN_P^{\,t}}{D} + 4N_P^t\right) \frac{\rho V^2}{2} \tag{A.7}$$

Where f is the friction factor for fully developed fluid flow. For fully developed laminar flow, f is obtained from:

$$f = 64/Re \tag{A.8}$$

And for fully developed turbulent flow, f is calculated by Eq. (B.3).

The pressure drop of two phase fluid flows inside the tubes is the sum of the static pressure drop ΔP_{stat}, the momentum pressure drop ΔP_{mom} and the frictional pressure drop ΔP_{frict}:

$$\Delta P_{tube_{2pH}} = \Delta P_{stat} + \Delta P_{mom} + \Delta P_{frict} \tag{A.9}$$

The static pressure drop ΔP_{stat}, is zero because of the no change in static head for a horizontal tube, i.e. $H = 0$ so:

$$\Delta P_{stat} = \rho_{tp} g H \sin\theta = 0 \tag{A.10}$$

The momentum pressure drop ΔP_{mom}, as described by Didi et al. [41] is calculated using a void fraction obtained from the drift flux model:

$$\Delta P_{mom} = G\left\{\frac{(1-x)^2}{\rho_l(1-\varepsilon)} + \frac{x^2}{\rho_v \varepsilon}\right\}_{x_{in}}^{x_{out}} \tag{A.11}$$

Where ε is the void fraction, is obtained from the Steiner version of the drift flux model of Rouhani and Axelsson [42] for horizontal tubes:

$$\varepsilon = \frac{x}{\rho_v}\left\{\left[1 + 0.12(1-x)\right]\left(\frac{x}{\rho_v} + \frac{1-x}{\rho_l}\right) + \frac{1.18\left(1-x\right)\left[g\sigma\left(\rho_l - rho_v\right)\right]^{0.25}}{G\rho_l^{\,0.5}}\right\}^{-1} \tag{A.12}$$

And the frictional pressure drop ΔP_{frict} is obtained from integral of the two phase frictional pressure gradient that is calculated by the correlation of Müller-Steinhagen and Heck [43]:

$$\Delta P_{frict} = \int_0^Z \left(\frac{dP}{dZ}\right)_{frict} dZ = \left\{-\frac{3}{4}(1-x)^{4/3}\left[a + 2(b-a)x\right] + \frac{1}{4}bx^4 - \frac{9}{14}(b-a)(1-x)^{7/3}\right\}_{x_{in}}^{x_{out}} \tag{A.13}$$

where a and b are the frictional pressure gradients when all the flow is assumed liquid and vapor, respectively:

$$a = \left(\frac{dp}{dz}\right)_{lo} = f_l \frac{2G^2}{d_i \rho_l} \tag{A.14}$$

$$b = \left(\frac{dp}{dz}\right)_{vo} = f_v \frac{2G^2}{d_i \rho_v} \tag{A.15}$$

And the friction factors, f_l and f_v, are calculated from the corresponding Reynolds number by:

$$f = \frac{0.079}{Re^{0.25}} \tag{A.16}$$

Appendix B. Heat transfer calculations

The Colburn j-factor for an ideal tube bank is calculated by:

$$j_i = a_1 \left(\frac{1.33}{P_T/d_o}\right)^a (Re_s)^{a_2} \tag{B.1}$$

where the constants a_1, a_2, a_3 and a_4 are given in Ref. [35]. And the constant a is defined by:

$$a = \frac{a_3}{1 + 0.14(Re_s)^{a_4}} \tag{B.2}$$

The correlation of Petukhov [44] for the smooth tube which is used to obtain the friction factor in the Eq. (44) at $10^4 \le Re \le 5 \times 10^6$, is:

$$f = \left[0.790 \ln(Re) - 1.64\right]^{-2} \tag{B.3}$$

Single phase liquid flow heat transfer coefficient, h_l, is calculated by the Dittus-Boelter [45] correlation:

$$h_l = 0.023\left[G\left(1-x\right)\frac{D}{\mu_l}\right]^{0.8} \frac{(Pr)^{0.4} k_l}{D} \tag{B.4}$$

where G is the mass velocity; x is the vapor quality.

E is the enhancement factor:

$$E = 1 + 3000\, Bo^{0.86} + 1.12\left(\frac{x}{1-x}\right)^{0.75}\left(\frac{\rho_l}{\rho_v}\right)^{0.41} \tag{B.5}$$

which is corrected for mixture effects utilizing Thome [46] nucleate pool boiling equation as described in Ref. [47].

$$F_C = \left\{1 + \frac{h_l}{q}\Delta T_{glide}\left[1 - \exp\left(\frac{-B_o q}{\rho_l \Delta H_{vap} \beta_l}\right)\right]\right\}^{-1} \tag{B.6}$$

where h_l is the ideal heat transfer coefficient calculated with the Gungor-Winterton correlation without mixture effects, but with the mixture physical properties; ΔT_{glide} is the temperature glide; B_o is a scaling factor assumed to be 1.0 (i.e. the theory assumes all heat transfer at a bubble interface is latent heat); q is the local heat flux attributable to nucleate boiling; β_l is the liquid phase mass transfer coefficient that can be assumed to have a constant value of 0.0003 m/s.

And the boiling number, Bo, is calculated by:

$$Bo = \frac{q}{G\Delta H_{vap}} \tag{B.7}$$

At the correlation of Shah [38] regime I occurs when $J_v \geq 0.98(Z + 0.263)^{-0.62}$, where J_v is the dimensionless vapor velocity defined by:

$$J_v = xG/\left[gD\rho_v(\rho_l - \rho_v)\right]^{0.5} \tag{B.8}$$

h_I and h_{Nu} are calculated by the following correlations:

$$h_I = h_{LS}\left(1 + \frac{3.8}{Z^{0.95}}\right)\left(\frac{\mu_l}{14\mu_v}\right)^{(0.0058+0.557p_r)} \tag{B.9}$$

$$h_{Nu} = 1.32\, Re_{LS}^{(-1/3)}\left[\frac{\rho_l(\rho_l - \rho_v)g(k_l)^3}{(\mu_l)^2}\right]^{1/3} \tag{B.10}$$

where h_{LS} is the heat transfer coefficient assuming liquid phase flowing alone in the tube, and it is calculated by Dittus-Boelter [45] correlation:

$$h_{LS} = 0.023(Re_{LS})^{0.8}(Pr_l)^{0.4}\frac{k_l}{D} \tag{B.11}$$

And Z is Shah's correlating parameter calculated by:

$$Z = \left(\frac{1}{x} - 1\right)^{0.8}(p_r)^{0.4} \tag{B.12}$$

References

[1] J. Bao, L. Zhao, A review of working fluid and expander selections for organic Rankine cycle, Renew. Sustain Energy Rev. 24 (2013) 325–342.
[2] B.F. Tchanche, M. Pétrissans, G. Papadakis, Heat resources and organic Rankine cycle machines, Renew. Sustain Energy Rev. 39 (2014) 1185–1199.
[3] E.H. Wang, H.G. Zhang, B.Y. Fan, M.G. Ouyang, Y. Zhao, Q.H. Mu, Study of working fluid selection of organic Rankine cycle (ORC) for engine waste heat recovery, Energy 36 (2011) 3406–3418.
[4] G.Q. Shu, X.N. Li, H. Tian, X.Y. Liang, H.Q. Wei, X. Wang, Alkanes as working fluids for high-temperature exhaust heat recovery of diesel engine using organic Rankine cycle, Appl. Energy 119 (2014) 204–217.
[5] H. Tian, G.Q. Shu, H.Q. Wei, X.Y. Liang, L.N. Liu, Fluids and parameters optimization for the organic Rankine cycles (ORCs) used in exhaust heat recovery of internal combustion engine (ICE), Energy 47 (1) (2012) 125–136.
[6] R. Chacartegui, D. Sanchez, J.M. Munoz, T. Sanchez, Alternative ORC bottoming cycles for combined cycle power plants, Appl. Energy 86 (10) (2009) 2162–2170.
[7] J.P. Roy, M.K. Mishra, A. Misra, Performance analysis of an Organic Rankine Cycle with superheating under different heat source temperature conditions, Appl. Energy 88 (2011) 2995–3004.
[8] M. Chys, M. van den Broek, B. Vanslambrouck, M. De Paepe, Potential of zeotropic mixtures as working fluids in organic Rankine cycles, Energy 44 (1) (2012) 623–632.
[9] J.L. Wang, L. Zhao, X.D. Wang, A comparative study of pure and zeotropic mixtures in low-temperature Rankine cycle, Appl. Energy 87 (11) (2010) 3366–3373.
[10] F. Heberle, M. Preiinger, D. Brüggemann, Zeotropic mixtures as working fluids in organic Rankine cycles for low-enthalpy geothermal resources, Renew. Energy 37 (1) (2012) 364–370.
[11] C.J. Bliem, Zeotropic Mixtures of Halocarbons as Working Fluids in Binary Geothermal Power Generation Cycles, EG and G Idaho, Inc., Idaho Falls (USA), 1987.
[12] G.Q. Shu, Y. Gao, H. Tian, H.Q. Wei, X.Y. Liang, Study of mixtures based on hydrocarbons used in ORC (Organic Rankine Cycle) for engine waste heat recovery, Energy 74 (2014) 428–438.
[13] W. Li, X. Feng, L.J. Yu, J. Xu, Effects of evaporating temperature and internal heat exchanger on organic Rankine cycle, Appl. Therm. Eng. 31 (17–18) (2011) 4014–4023.
[14] P.J. Mago, L.M. Chamra, K. Srinivasan, C. Somayaji, An examination of regenerative organic Rankine cycles using dry fluids, Appl. Therm. Eng. 28 (2008) 998–1007.
[15] G. Pei, J. Li, J. Ji, Analysis of low temperature solar thermal electric generation using regenerative organic Rankine cycle, Appl. Therm. Eng. 30 (8–9) (2010) 998–1004.
[16] J.P. Roy, M.K. Mishra, A. Misra, Parametric optimization and performance analysis of a waste heat recovery system using organic Rankine cycle, Energy 35 (12) (2010) 5049–5062.
[17] M. Yari, Performance analysis of the different Organic Rankine Cycles (ORCs) using dry fluids, Int. J. Exergy 6 (2009) 323–342.
[18] I.H. Aljundi, Effect of dry hydrocarbons and critical point temperature on the efficiencies of organic Rankine cycle, Renew. Energy 36 (2011) 1196–1202.
[19] S. Quoilin, S. Declaye, B.F. Tchanche, V. Lemort, Thermo-economic optimization of waste heat recovery Organic Rankine Cycles, Appl. Therm. Eng. 31 (2011) 2885–2893.
[20] E. Cayer, N. Galanis, H. Nesreddine, Parametric study and optimization of a transcritical power cycle using a low temperature source, Appl. Energy 87 (2010) 1349–1357.
[21] Z. Shengjun, W. Huaixin, G. Tao, Performance comparison and parametric optimization of subcritical organic Rankine cycle (ORC) and transcritical power cycle system for low-temperature geothermal power generation, Appl. Energy 88 (8) (2011) 2740–2754.
[22] L. Xiao, S.Y. Wu, T.T. Yi, Li YR. Liu Ch, Multi-objective optimization of evaporation and condensation temperatures for subcritical organic Rankine cycle, Energy 83 (2015) 723–733.
[23] ⟨http://www.cat.com/en_US/power-systems/marine-power-systems/commercial-propulsion-engines/18493267.html⟩, May 28, 2015.

[24] S. Quoilin, M. van den Broek, S. Declaye, P. Dewallef, V. Lemort, Techno-economic survey of Organic Rankine Cycle (ORC) systems, Renew. Sustain Energy Rev. 22 (2013) 168–186.
[25] E.W. Lemmon, M.L. Huber, M.O. McLinden, NIST standard reference database 23: reference fluid thermodynamic and transport properties-REFPROP. 8.0, 2007.
[26] R. Turton, R.C. Bailie, W.B. Whiting, J.A. Shaeiwit, Analysis, Synthesis, and Design of Chemical Processes, Pearson Education Inc., 2009.
[27] S. Jenkins, Economic indicators: CEPCI, Chemical Engineering Essentials for the CPI Professional. ⟨http://www.chemengonline.com/economic-indicators-cepci/?printmode=1⟩, March 19, 2015.
[28] W.D. Seider, J.D. Seader, D.R. Lewin, Product and Process Design Principles: Synthesis, Analysis, and Evaluation, John Wiley, 2003.
[29] A. Bejan, G. Tsatsaronis, M. Moran, Thermal Design and Optimization, John Wiley & Sons, 1996.
[30] Power Purchase Price from clean and renewable sources: Minister of Energy, Renewable Energy Organization of Iran (SUNA).⟨http://www.suna.org.ir/en/guaranteed⟩, July 21, 2015.
[31] K. Thulukkanam, Heat Exchanger Design Handbook, Second edition, . CRC Press, Taylor & Francis Group, 2013.
[32] E.E. Ludwig, Applied Process Design For Chemical And Petrochemical Plants, Third edition, . Gulf Professional Publishing, 1997.
[33] Tubular exchanger manufacturers association. Standards of tubular exchanger manufacturers association. TEMA, 1959.
[34] K.J. Bell, Delaware method for shell-side design, in: R.K. Shah, E.C. Subbarao, R.A. Mashelkar (Eds.), Heat Transfer Equipment Design, Hemisphere Publishing Corporation, 1988, p. 828.
[35] S. Kakac, H. Liu, A. Pramuanjaroenkij, Heat Exchangers: Selection, Rating, and Thermal Design, 2nd ed. CRC Press, 2002.
[36] V. Gnielinski, New equations for heat and mass transfer in turbulent pipe and channel flow, Int. Chem. Eng. 16 (1976) 359–368.
[37] K.E. Gungor, R.H.S. Winterton, Simplified general correlation for saturated flow boiling and comparisons of correlations with data, Can. J. Chem. Eng. 65 (1) (1987) 148–156.
[38] M.M. Shah, An improved and extended general correlation for heat transfer during condensation in plain tubes, HVACR Res. 15 (5) (2009) 889–913.
[39] K.J. Bell, M.A. Ghaly, An approximate generalized method for multicomponent partial condenser. In: American Institute of Chemical Engineers Symposium, vol. 69, 1973. pp. 72–79.
[40] V.L. Le, A. Kheiri, M. Feidt, S. Pelloux-Prayer, Thermodynamic and economic optimizations of a waste heat to power plant driven by a subcritical ORC (Organic Rankine Cycle) using pure or zeotropic working fluid, Energy 78 (2014) 622–638.
[41] M.B. Ould Didi, N. Kattan, J.R. Thome, Prediction of two-phase pressure gradients of refrigerants in horizontal tubes, Int. J. Refrig. 25 (7) (2002) 935–947.
[42] S.Z. Rouhani, E. Axelsson, Calculation of void volume fraction in the subcooled and quality boiling regions, Int. J. Heat. Mass Transf. 13 (2) (1970) 383–393.
[43] H. Müller-Steinhagen, K. Heck, A simple friction pressure drop correlation for two-phase flow in pipes, Chem. Eng. Process.: Process Intensif. 20 (6) (1986) 297–308.
[44] B.S. Petukhov, Heat transfer and friction in turbulent pipe flow with variable physical properties, Adv. Heat. Transf. 6 (1970) 503–564.
[45] F.W. Dittus, L.M.K. Boelter, Heat Transfer in Automobile Radiators of the Tubular Type, University of California Press, 1930.
[46] J.R. Thome, Prediction of the mixture effect on boiling in vertical thermosyphon reboilers, Heat. Transf. Eng. 10 (2) (1989) 29–38.
[47] N. Kattan, D. Favrat, J.R. Thome, Re502 and two near-azeotropic alternatives. Part I: intube flow boiling tests. ASHRAE winter meeting, Chicago, symposium CH-95-12 ASHRAE Trans 1995, 101(1), 1–36. Paper CH-95-12-3.